

# **Shrinkage Cracking Propensity of Ultra-High Performance Concrete**

**Igor De la Varga<sup>1</sup>, Robert P. Spragg<sup>1</sup>, Rafic G. El-Helou<sup>2</sup>, Benjamin A. Graybeal<sup>3</sup>**

<sup>1</sup>*SES Group and Associates, FHWA-Turner Fairbank Highway Research Center, McLean, VA.*

<sup>2</sup>*National Research Council Associate, FHWA-Turner Fairbank Highway Research Center, McLean, VA.*

<sup>3</sup>*Federal Highway Administration, FHWA-Turner Fairbank Highway Research Center, McLean, VA.*

## **Abstract**

It is widely accepted that ultra-high performance concrete (UHPC) provides better mechanical and durability properties than high performance or conventional concrete. The high cementitious materials and fiber contents are key to its change in properties, making this type of material suitable for a wide range of structural applications. However, because of its very low water-to-cementitious materials ratio range (i.e, 0.18-0.22) compared to that of high strength and/or conventional concrete (typically higher than 0.30), this type of material can be more prone to autogenous shrinkage cracking. This paper will examine the shrinkage cracking propensity of several commercially-available UHPC materials compared to that of a typical high strength concrete, a conventional concrete, and a cementitious grout. A dual ring test will be used for this purpose, which offers the possibility to not only assess the tensile stress developed in the material due to restrained autogenous shrinkage, but also to estimate the stress reserve capacity of the materials (that is, how near the materials are to cracking). The results will help UHPC designers and end users better understand the cracking behavior of these materials under restrained conditions.

**Keywords: UHPC, Concrete, Cementitious Grout, Shrinkage Cracking, Dual Ring Test, Tensile Stress, Modulus of Elasticity**

## **1. Background**

Ultra-high performance concrete (UHPC) is a special type of concrete that has become more popular over the last two decades due to the enhanced mechanical and durability properties compared to those of conventional concrete [1–7]. UHPC contains larger amounts of cement and cementitious materials compared to conventional concrete, along with a well-graded aggregate system consisting only of very fine particles such as inert silica flour and other fillers (that is, coarse aggregates are not used in UHPC). The successful design of UHPC materials is based on an optimized particle packing of both cementitious and fine aggregate systems, the use of low amounts of water, and the addition of the appropriate chemical admixture system (e.g., superplasticizer, accelerators, viscosity modifier agents, etc.). Steel or other type of fibers are commonly added in volumes ranging 1 to 3 %.

Despite the higher initial material cost, transportation agencies are now more receptive to its use given the outstanding mechanical and durability properties, which should provide an increase in the infrastructure service life. UHPC was initially used in connections between prefabricated bridge elements (PBE) replacing conventional cementitious grouts [8–13]. The material volume needed in this type of application was small enough to justify the higher material costs. However, interest has grown over the years as more applications for UHPC are being

identified, including bridge repair and rehabilitation [14,15] as well as bridge deck overlays [16–18]. In some cases, primary structural elements have been exclusively fabricated with UHPC [19]. In all these applications, it is crucial that the material offers superior mechanical and durability properties. Strong and durable materials tend to exhibit less cracking. As such, it is important to understand the inherent cracking behavior of UHPC-class materials.

Cracking in cementitious materials is a common occurrence, especially in concretes with lower water-to-cementitious materials ratios ( $w/cm$ ) [20,21]. Lowering the  $w/cm$  while adding high range water reducing admixtures is a common practice to develop high performance concretes. As mentioned earlier, UHPC follows this same approach. Low  $w/cm$  concretes are more prone to early-age cracking due to three effects: 1) increased temperature rise shortly after placement due to the high cement contents, 2) increased plastic shrinkage cracking due to reduced bleeding rates, and 3) increased autogenous shrinkage [22]. While plastic shrinkage and thermal volume changes have been recognized in concrete construction over the last several decades and methodologies have been developed to deal with these effects, autogenous shrinkage is a problem that has gained attention more recently [23–25].

Autogenous shrinkage is a deformation not caused by external influences (i.e., moisture transfer or temperature changes). Rather, autogenous shrinkage can be thought of as an ‘internal drying’ caused by the hydration reactions and their accompanying chemical shrinkage. Chemical shrinkage occurs when cement reacts with water as the reacted products occupy a smaller volume than the initial constituents [26,27]. In fluid systems (e.g., prior to set), this chemical shrinkage does not cause much concern and the entire system collapses on itself resulting in an externally measured volume change that is equal to the chemical shrinkage. However, after the concrete begins to harden, the structure of the cementitious matrix does not enable the externally measured volume change to be equal to the volume of chemical shrinkage [28]. As a result, vapor filled spaces are created within the matrix (i.e., internal drying) and stress begins to develop in the hardening paste [29]. If stresses reach the tensile strength of the material, cracking will occur [23].

This paper will examine the shrinkage cracking propensity of several commercially-available UHPC materials compared to that of a typical high strength concrete, a conventional concrete, and a cementitious grout. A dual ring test will be used. Important mechanical properties needed to better explain the cracking behavior will also be assessed, namely tensile strength and modulus of elasticity.

## **2. Materials**

### **2.1. UHPCs**

Four commercially-available UHPC materials were used in the study. They are labelled as U1, U2, U3, and U4 throughout the paper. The mixing proportions used were those recommended by the different UHPC suppliers. In all of them, the pre-blended powder formulation is unknown and the fiber volume is 2 %.

Material U1 consisted of a pre-blended, pre-bagged powder mixture containing all of the solids (with the exception of fibers), a 3-component chemical admixture system, and steel fiber reinforcement with a nominal length of 13 mm (0.5 inches) and a nominal diameter of 0.2 mm (0.008 inches). The tensile strength of the fibers, as reported by the manufacturer, was 3,750 MPa (399 ksi).

Material U2 consisted of a pre-blended powder mixture containing all of the solids (with the exception of fibers), a 2-component chemical admixture system, and steel fiber reinforcement. U2 employed two types of fibers: straight and hooked. The straight fibers had a nominal length of 20 mm (0.8 inches) and a nominal diameter of 0.2 mm (0.008 inches). The hooked fibers had a nominal length of 25 mm (1 inch) and a nominal diameter of 0.3 mm (0.012 inches). The tensile strength of the fibers, as reported by the manufacturer, was greater than 2,500 MPa (363 ksi).

Material U3 consisted of a pre-blended powder mixture containing all of the solids (with the exception of fibers); a 2-component chemical admixture system; and steel fiber reinforcement with a nominal length of 13 mm (0.5 inches) and a nominal diameter of 0.2 mm (0.008 inches). The tensile strength of the fibers, as reported by the manufacturer, was 3,750 MPa (399 ksi).

Material U4 consisted of a pre-blended powder mixture containing all of the solids and the chemical admixtures (with the exception of fibers); and steel fiber reinforcement with a nominal length of 13 mm (0.5 inches) and a nominal diameter of 0.2 mm (0.008 inches). The tensile strength of the fibers, as reported by the manufacturer, was 3,750 MPa (399 ksi).

## **2.2. High and Normal Strength Concretes**

Two concretes were used in the study. The concretes were made using local materials and following Virginia DOT requirements [30] to perform similarly to a A3 normal strength concrete (labelled here as C1), and a A4 high strength concrete (labelled as C2). Both concretes were prepared using ordinary portland cement, ASTM C150-16 Type I/II [31], with a Blaine fineness of 382 m<sup>2</sup>/kg, and a density of 3070 kg/m<sup>3</sup> (191 lbs/ft<sup>3</sup>). Class F fly ash with a specific gravity of 2.50 was also included in the concrete mixtures, replacing a mass cement fraction of 22 % and 35 % for the C1 and C2 concretes, respectively. The fine aggregate (FA) used was ordinary river sand with a SSD apparent specific gravity of 2.59. The coarse aggregate (CA) consisted of dolomitic limestone with a SSD apparent specific gravity of 2.85. C1 was designed with a water-to-cementitious materials ratio (*w/cm*) of 0.49 by mass, cement+fly ash:FA:CA ratio of 1:1.6:3.3 (by mass), a minimum slump of 190 mm (7.5 inches) per ASTM C143 [32], air content of 5.5 % (achieved by using a high-range water reducer) per ASTM C231 [33], and a minimum specified 28-d compressive strength of 21 MPa (3,000 psi). C2 was designed with a *w/cm* of 0.43 by mass, cement+fly ash:FA:CA ratio of 1:1.8:2.8 (by mass), a minimum slump of 140 mm (5.5 inches) (achieved by using a high-range water reducer) per ASTM C143, air content of 5.5 % (achieved by using a high-range water reducer) per ASTM C231, and a targeted 28-d compressive strength of 28 MPa (4,000 psi).

## **2.3. Cementitious Grout**

Given the widespread use of ‘non-shrink’ cementitious grouts in prefabricated bridge element connections [12], a commercially-available cementitious grout was also used in the study, labelled here as G1. The grout was supplied in a bag containing the solid fraction (e.g., cementitious materials, additives, and fine aggregates) that is mixed with a certain amount of water following the manufacturer’s recommendations to obtain an average flow of 100 % ± 2 % per ASTM C1437. The grout material required a water-to-solids ratio (*w/s*) of 0.16 by mass and produced a 28-d compressive strength of 62 MPa (9,000 psi). It is worthwhile to mention that a *w/s* of 0.16 corresponds to a *w/cm* of about 0.55, considering that approximately 30 % of the solid components of this grout are reactive [34].

### 3. Testing Methods

#### 3.1. Dual Ring Test

Cracking propensity was assessed using a dual ring test (DRT) [35,36]. The DRT is an extension of the concepts of the commonly used single ring shrinkage test, described in ASTM C1581 [37]. An AASHTO specification describing the DRT test has recently been developed [38]. The DRT consists of two concentric Invar steel rings that allow for the measurements of both shrinkage and expansion with approximately a 72 % degree of restraint. The DRT operates by casting a 38-mm (1.50-inch) thick annulus of the testing material between the two restraining rings. The temperature of the test was controlled by placing copper tubing that is connected to a water/ethyl-glycol system on both the top and bottom of the rings and sample. Due to the low coefficient of thermal expansion of the Invar rings, the DRT has the ability to retain a stable degree of restraint over varying temperatures. The rings, sample, and temperature control coil were sealed in a heavily insulated chamber. The temperature of the water/ethyl-glycol mixture was controlled through an external water bath. The rings were instrumented with four equally spaced Invar strain gages that measure the strain developed in the inner and outer restraining rings. Thermocouples were also used to measure the rings and sample temperature. A data acquisition system was set up so that the strain and temperature of the rings were recorded every 30 sec. Figure 1 shows the complete setup. The recorded strains were used to calculate the residual stress accumulation in the sample [36,38]. The induced stresses from temperature changes can be used to show the stress reserve capacity and determine how near the specimen is to cracking. In this study, isothermal conditions at  $23 \pm 0.1$  °C ( $73.4 \pm 0.2$  °F) were maintained for 7 days, at which time the temperature was reduced at a rate of 2 °C/h (3.6 °F/h) down to  $-21$  °C ( $-5.8$  °F) to induce cracking in the material. Cracking in this test is detected by a sudden drop in the strain (and thus stress) reading. In fiber reinforced cement-based materials, microcracking is expected in the form of small sudden drops in the stress readings. This will be further discussed in the results section.

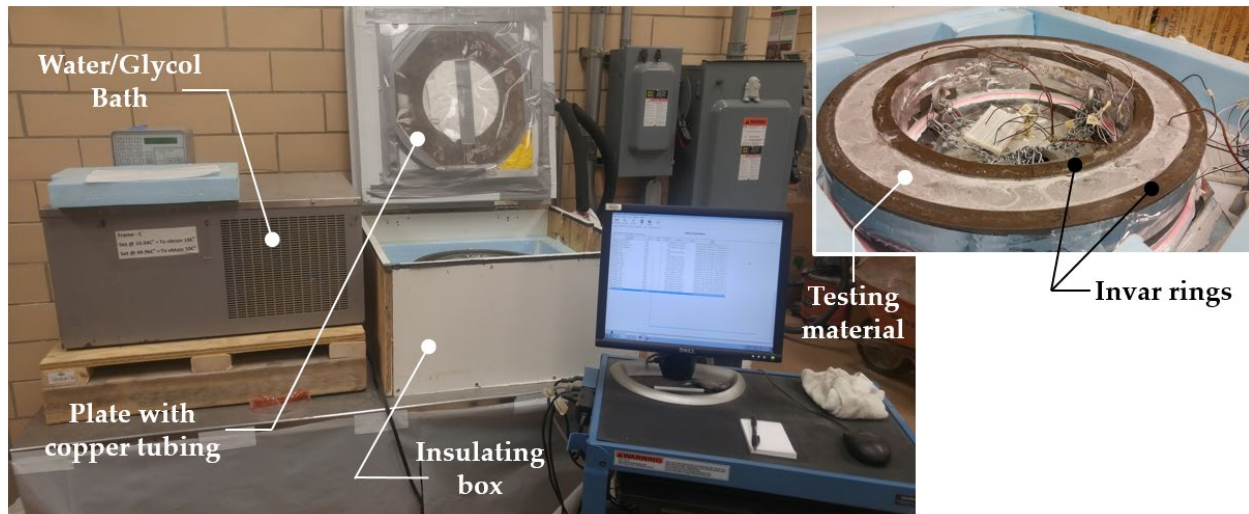


Figure 1. Dual ring test (DRT) setup

#### 3.2. Tensile Strength

Tensile strength was assessed using two different test methods. For the UHPC specimens, tests were performed according to a direct tension test developed by Graybeal and Baby [39]. A minimum of six specimens per material were prepared and cured in laboratory conditions of  $23 \pm$

2 °C (73.4 ± 3.6 °F) and 50 ± 8 % relative humidity until the testing age of 7 days. For the concrete and grout specimens, ASTM C496-17 was used [40], which allows for the determination of the splitting (indirect) tensile strength of a cylindrical concrete specimen. Three specimens per material were prepared and sealed-cured in plastic bags at laboratory conditions of 23 ± 2 °C (73.4 ± 3.6 °F) until the testing age of 7 days. 7 days was selected as testing age to be correlated to the DRT results, where cracking was induced in the specimens after 7 days of isothermal and sealed conditions.

### **3.3. Elastic Modulus**

The elastic modulus was determined using also two different test methods. The UHPC specimens were tested in accordance with ASTM C1856-17 [41], whereas the concrete and grout specimens were tested via ASTM C469-14 [42]. Three 102-mm (4-inch) diameter by 204-mm (8-inch) tall cylindrical specimens of each material were prepared and sealed-cured in plastic bags for 7 days at laboratory conditions of 23 ± 2 °C (73.4 ± 3.6 °F). The test cylinder was fixed in a compressometer housing LVDTs to measure axial deformations. The test cylinders were loaded three times at a rate of 1 MPa/sec (145 psi/sec) for the UHPC materials, and 0.25 MPa/sec (35 psi/sec) for the concrete and grout materials. The first loading was disregarded and the average of the last two loadings was recorded. The calculation of the elastic modulus was done using a fitted line on the stress-strain response up to 40 % of the ultimate load.

## **4. Results and Discussion**

As already mentioned, cementitious materials undergo volume changes (primarily shrinkage) freely in unrestrained conditions, without inducing significant stress in the material. However, structural cementitious materials are commonly connected to other stationary elements (e.g., reinforcement bars, other previously cast concrete elements, etc.) that do not experience the same volume change, thereby limiting the volume change that the particular cementitious material of interest can experience without developing stresses. The DRT used in this study was designed to subject the material to a 72 % degree of restraint, similar to values seen in reinforced concrete bridge decks whose free movement is restrained by reinforcement and other elements of the structural system (e.g., girders, reinforcement). This particular degree of restraint in the DRT is similar to that of the commonly used single ring test described in ASTM C1581 [37], which was designed with that degree of restraint under the same assumptions. High degrees of restraint could induce cracking in certain conditions, causing both strength and durability issues. Figures 2 and 3 show the residual stress generated in the different materials when tested in the DRT for 7 days under sealed isothermal conditions of 23 ± 0.01 °C (73.4 ± 0.02 °F). The stresses were calculated from the strains measured on both inner and outer rings using the equations described in the AASHTO standard [38]. The residual stresses were zeroed at the final setting time of each of the materials tested.

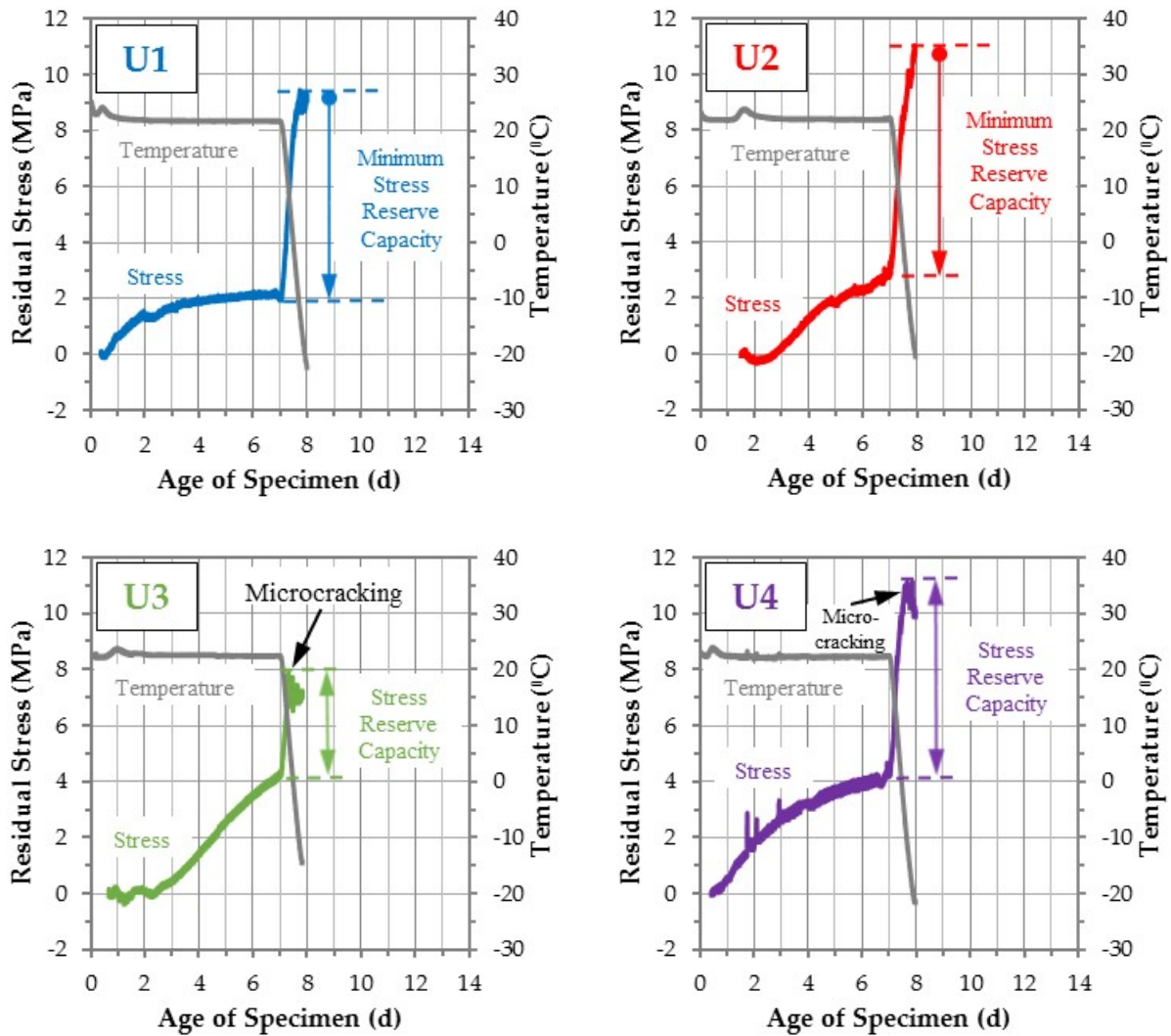
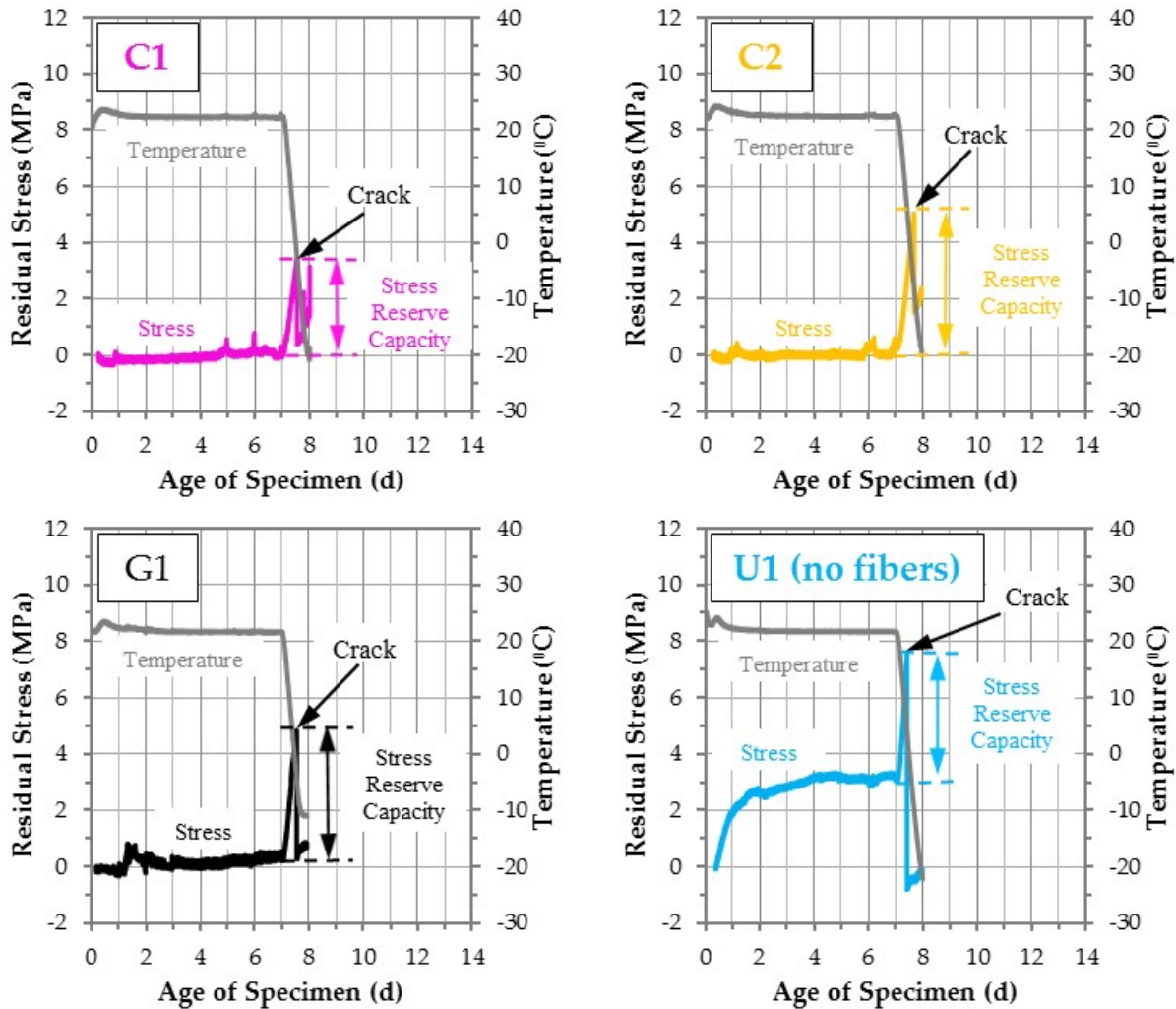


Figure 2. Residual stress development and stress reserve capacity of the UHPC materials tested in the study.

As observed in the figures, all U specimens developed larger residual stress values during the 7-d isothermal period compared to C1, C2, and G1, which exhibited negligible residual stress development. This makes sense as C1, C2, and G1 were designed with  $w/cm$  of 0.49, 0.43, and about 0.55. According to Powers model [29], cementitious systems with  $w/cm$  lower than 0.42 are more prone to develop self-desiccation (i.e., internal drying due to autogenous shrinkage), thus developing internal (shrinkage) stresses that may lead to cracking. U1, U2, U3, and U4 are designed with  $w/cm$  of about 0.20, thereby developing higher tensile stresses of about 2 MPa (290 psi), 3 MPa (435 psi), and 4 MPa (580 psi), respectively, before the temperature was purposely reduced at 7 days to induce cracking in the specimens.



**Figure 3. Residual stress development and stress reserve capacity of the concrete and grout materials tested in the study.**

An additional U1 specimen was prepared without adding steel fibers in order to assess the role of the fibers in reducing shrinkage stress development. It was observed that U1 without fibers developed approximately two times the residual stress compared to the comparable material with fibers, with the majority of the residual stress development occurring during the first 2-3 days when the material is still developing tensile strength and thus is less able to resist cracking. This higher residual stress development may lead to shrinkage cracking. In fact, the U1 specimen without fibers cracked when the temperature was reduced, indicated by a sudden drop in the stress reading at about 7.5 days. U1 and U2 specimens did not crack even when the temperature dropped to -21 °C (-5.8 °F), as no sudden drop in the stress curve was detected. However, U3, U4, C1, C2, and G1 did crack when the temperature was reduced. While both concretes and grout materials were expected to crack given their lower tensile strength compared to UHPC materials (see results in Table 1), it was unexpected to see that the U3 and U4 specimens also cracked. This might have been partly caused by the fact that these two materials developed a substantial residual stress during the 7-d isothermal period (about 4 MPa (580 psi)). Although not included in this study, unrestrained shrinkage was previously measured on U3, showing larger values compared to other commercially-available UHPC materials, including U1 [43]. A photo of a typical thermally-

induced crack observed in the C1, C2, G1, or U1 (without fibers) specimens is shown in Figure 4. U3 and U4 did not show an individual crack, at least not visible to the naked eye. So, microcracking is expected to have occurred in these specimens. In fact, the residual stress curve shows subsequent drops (see Figure 2), rather than one single sudden drop. This is an indication that the fibers are ‘bridging’ microcracks as they occur.

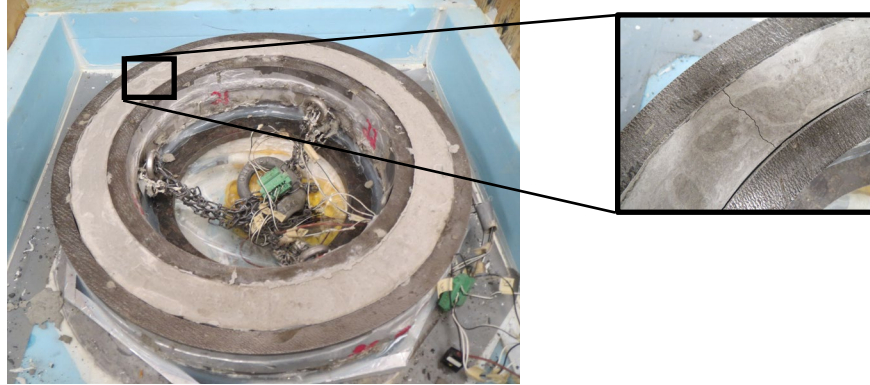


Figure 4. Typical individual crack observed in the C1, C2, G1, or U1 (without fibers) ring specimens.

Table 1 shows the tensile strength, elastic modulus, cracking temperature, and stress reserve capacity of the materials tested. The latter would identify how near the materials are to cracking by calculating the difference between the stress developed at 7 days and the maximum stress reached when the temperature in the rings was reduced. As observed, U1, U2, and U4 materials exhibited considerably higher stiffness (i.e., elastic modulus) and tensile strength compared to the concretes and grout materials. Higher tensile properties, along with a good fiber reinforcement system, should help in reducing or even preventing cracking. The calculated stress reserve capacity confirms this statement. In fact, only a minimum value could be calculated for U1 and U2 as the specimens did not crack (indicated by the dot-and-arrow on the plots, and with the “greater than” symbol in Table 1). It is interesting to note that, among the UHPC materials, U3 showed lower mechanical properties. This, along with the higher shrinkage observed elsewhere [43], may explain the lower stress reserve capacity and the cracking occurrence when reducing the temperature in the DRT. In terms of shrinkage cracking, U3 behaves similarly to C1, C2, and G1. Even so, it is expected that U3 would still perform differently than conventional materials when deployed in practice due to its post-peak behavior (i.e., sustained tensile load capacity).

Table 1. Tensile strength, elastic modulus, cracking temperature, and stress reserve capacity of the materials tested in the study.

	U1	U2	U3	U4	C1	C2	G1
<b>7d Elastic Modulus (GPa)</b>	42.3 (0.7)	42.6 (2.1)	32.3 (1.6)	45.4 (0.3)	19.1 (0.4)	22.0 (0.2)	27.4 (0.3)
<b>7d Tensile Strength (MPa)</b>	7.5 (0.5)	7.1 (0.5)	6.5 (1.1)	9.7 (0.7)	3.0 (0.7)	2.6 (0.4)	3.7 (0.4)
<b>Cracking Temperature in DRT (°C)</b>	N/A	N/A	6.9	-5.0	-3.4	-7.1	-4.1
<b>Stress Reserve Capacity (MPa)</b>	>7.4	>7.8	3.6	5.8	3.4	4.6	4.5

Note: 1 GPa = 1000 MPa = 145,038 psi

Note: Numbers in parenthesis represent ± one standard deviation from the average of three specimens, except for the UHPC tensile strength tests, where a minimum of six specimens were used.

## 5. Conclusions

The study presented in this paper shows results on shrinkage cracking propensity of UHPC materials compared to that of a conventional concrete, high strength concrete, and a cementitious grout. The cracking behavior was assessed using a dual ring test and other mechanical properties such as tensile strength and elastic modulus. It can be concluded that, while developing higher shrinkage stresses than conventional concretes or grouts, UHPC materials offer higher stress reserve capacity, which translates to less shrinkage cracking propensity. If cracking occurs, it would be in the form of microcracks thanks to the presence of fibers in the system.

## 6. References

- [1] B.A. Graybeal, Compression Testing of Ultra-High-Performance Concrete, *Adv. Civ. Eng. Mater.* 4 (2014) 20140027. doi:10.1520/ACEM20140027.
- [2] B.A. Graybeal, Tensile Mechanical Response of Ultra-High-Performance Concrete, *Adv. Civ. Eng. Mater.* 4 (2014) 20140029. doi:10.1520/ACEM20140029.
- [3] B. Graybeal, J. Tanesi, Durability of an Ultrahigh-Performance Concrete, *J. Mater. Civ. Eng.* 19 (2007) 848–854. doi:10.1061/(ASCE)0899-1561(2007)19:10(848).
- [4] B.H. Green, R.D. Moser, D.A. Scott, W.R. Long, Ultra-High Performance Concrete History and Usage by the Corps of Engineers, *Adv. Civ. Eng. Mater.* 4 (2015) 132–143. doi:10.1520/ACEM20140031.
- [5] E. Fehling, Ultra high performance concrete (UHPC), in: *Proc. Int. Symp. Ultra High Perform. Concr.*, 2004: p. 868. <http://www.upress.uni-kassel.de/katalog/abstract.php?978-3-89958-376-2>.
- [6] B.A. Graybeal, Material Property Characterization of Ultra-High Performance Concrete, FHWA-HRT-06-103, Washington DC, 2006.
- [7] I. De la Varga, Z. Haber, J. Yuan, B.A. Graybeal, Material Property Evaluation of Different Commercially-Available UHPC-Class Materials, in: *First Int. Intercative Symp. UHPC*, Des Moines, IA, 2016. doi:10.21838/uhpc.2016.106.
- [8] B.A. Graybeal, Ultra-high-performance concrete connections for precast concrete bridge decks, *PCI J.* (2014) 48–62.
- [9] J. Charron, D. Ph, P. Eng, B. Massicotte, D. Ph, P. Eng, Design and Behavior of UHPFRC Field-Cast Transverse Connections between Precast Bridge Deck Elements, *J. Bridg. Eng.* 22 (2017) 1–11. doi:10.1061/(ASCE)BE.1943-5592.0001064.
- [10] J.K. Lee, S.H. Lee, Flexural behavior of ultra-high-performance fiber-reinforced concrete moment connection for precast concrete decks, *ACI Struct. J.* 112 (2015) 451–462. doi:10.14359/51687657.
- [11] M.P. Culmo, Accelerated Bridge Construction - Experience in Design, Fabrication and Erection of Prefabricated Bridge Elements and Systems (No. FHWA-HIF-12-013), Federal Highway Administration - U.S. Department of Transportation, McLean (VA), USA, 2011. <http://www.fhwa.dot.gov/bridge/abc/docs/abcmanual.pdf> (accessed August 31, 2016).
- [12] M.P. Culmo, Connection Details for Prefabricated Bridge Elements and Systems (No. FHWA-IF-09-010), Federal Highway Administration - U.S. Department of Transportation, McLean (VA), USA, 2009. <http://www.fhwa.dot.gov/bridge/prefab/if09010/report.pdf>.
- [13] B. Graybeal, Z. Haber, I. De la Varga, R. Spragg, Accelerated Construction of Robust Bridges through Material and Detailing Innovations, in: *Proc. 9th Int. Conf. Bridg. Maintenance, Safety, Manag.*, International Association for Bridge Maintenance and Safety,

- Melbourne, Australia, 2018.
- [14] M.A. Carbonell, *Compatibility of Ultra High Performance Concrete As Repair Material*, Michigan Technological University, 2012.
- [15] B. Massicotte, M.A. Dagenais, J.F. Garneau, *Bridge pier seismic strengthening using UHPFRC*, in: 9th Int. Conf. Short Mediu. Span Bridg., Calgary, Canada, 2014: pp. 1–15.
- [16] K. Habel, E. Denarié, E. Brühwiler, *Experimental investigation of composite ultra-high-performance fiber-reinforced concrete and conventional concrete members*, *ACI Struct. J.* 104 (2007) 93–101. doi:10.14359/18437.
- [17] Z.B. Haber, J.F. Munoz, I. De la Varga, B.A. Graybeal, *Bond characterization of UHPC overlays for concrete bridge decks: Laboratory and field testing*, *Constr. Build. Mater.* 190 (2018) 1056–1068. doi:10.1016/j.conbuildmat.2018.09.167.
- [18] Z.B. Haber, J.F. Munoz, I. De la Varga, B.A. Graybeal, *Ultra-High Performance Concrete for Bridge Deck Overlays* (No. FHWA-HRT-17-097), McLean, VA, 2017.
- [19] H. Russel, G. B.A. Graybeal, *Ultra-High Performance Concrete : A State-of-the-Art Report for the Bridge Community* (No. FHWA-HRT-13-060), Federal Highway Administration - U.S. Department of Transportation, McLean, VA, USA, 2013.
- [20] S.P. Shah, W.J. Weiss, *High performance concrete: strength, permeability, and shrinkage cracking*, in: *Proc. PCI/FHWA Int. Symp. High Perform. Concr.*, Orlando, FL, USA, 2000: pp. 331–340.
- [21] W.J. Weiss, W. Yang, S. Shah, *Factors influencing durability and early-age cracking in high strength concrete structures*, *High Performance Concrete: Research to Practice*, *ACI Spec. Publ.* 186 (1999) 387–409.
- [22] S.P. Shah, W.J. Weiss, W. Yang, *Shrinkage cracking in high performance concrete*, in: *Proc. PCI/FHWA Int. Symp. High Perform. Concr.*, New Orleans, LA, USA, 1997.
- [23] S.. Shah, W.. Weiss, W. Yang, *Shrinkage cracking - Can it be prevented?*, *ACI Concr. Int.* 20 (1998) 51–55. <https://www.concrete.org/publications/internationalconcreteabstractsportal/m/details/id/132>.
- [24] M.D. Brown, C.A. Smith, J.G. Sellers, K.J. Folliard, J.E. Breen, *Use of alternative materials to reduce shrinkage cracking in bridge decks*, *ACI Mater. J.* 104 (2007) 629–637.
- [25] D.P. Bentz, M.A. Peltz, *Reducing thermal and autogenous shrinkage contributions to early-age cracking*, *ACI Mater. J.* 105 (2008) 414–420. doi:10.14359/19904.
- [26] H. Le Chatelier, *Sur les changements de volume qui accompagnent le durcissement des ciments*, 5th ed., *Bulletin Société de l'Encouragement pour l'Industrie Nationale*, Paris, France, 1900.
- [27] R.G. L'Hermite, *Volume changes of concrete*, in: *4th Int. Symp. Chem. Cem.*, Washington DC, 1960.
- [28] G. Sant, P. Lura, J. Weiss, *Measurement of Volume Change in Cementitious Materials at Early Ages: Review of Testing Protocols and Interpretation of Results*, *Transp. Res. Rec. J. Transp. Res. Board.* 1979 (2006) 21–29. doi:10.3141/1979-05.
- [29] O.M. Jensen, P.F. Hansen, *Water-entrained cement-based materials: I. Principles and theoretical background*, *Cem. Concr. Res.* 31 (2001) 647–654. doi:10.1016/S0008-8846(01)00463-X.
- [30] *VDOT, Road and Bridge Specifications*, Virginia DOT, 2016.
- [31] *ASTM C150, Standard Specification for Portland Cement*, ASTM International, West Conshohocken (PA), USA, 2017. doi:10.1520/C0150.

- [32] ASTM C143, Standard Test Method for Slump of Hydraulic-Cement Concrete, ASTM International, West Conshohocken, PA, USA, 2015. doi:10.1520/C0143.
- [33] ASTM C231, Standard Test Method for Air Content of Freshly Mixed Concrete by the Pressure Method, West Conshohocken, PA, USA, 2010. doi:10.1520/C0231.
- [34] I. De la Varga, B.A. Graybeal, Dimensional Stability of Grout-Type Materials Used as Connections between Prefabricated Concrete Elements (No. FHWA-HRT-16-008), McLean, VA, 2016. <http://www.fhwa.dot.gov/publications/research/infrastructure/structures/bridge/16008/index.cfm>.
- [35] J.L. Schlitter, D.P. Bentz, W.J. Weiss, Quantifying stress development and remaining stress capacity in restrained, internally cured mortars, *ACI Mater. J.* 110 (2013) 3–11. doi:10.14359/51684361.
- [36] J.L. Schlitter, a H. Senter, D.P. Bentz, T. Nantung, W.J. Weiss, A Dual Concentric Ring Test for Evaluating Residual Stress Development due to Restrained Volume Change, *J. ASTM Int.* 7 (2010) 1–13. doi:10.1520/JAI103118.
- [37] ASTM C1581, Standard Test Method for Determining Age at Cracking and Induced Tensile Stress, ASTM International, West Conshohocken, PA, USA, 2013. doi:10.1520/C1581.
- [38] AASHTO T 363-17, Standard Method of Test for Evaluating Stress Development and Cracking Potential Due to Restrained Volume Change Using a Dual Ring Test Evaluating Stress Development and Cracking Potential Due to Restrained Volume Change Using a Dual Ring Test, American Association of State Highway and Transportation Officials, Washington DC, USA, 2017.
- [39] B.A. Graybeal, F. Baby, Development of direct tension test method for ultra-high-performance fiber-reinforced concrete, *ACI Mater. J.* 110 (2013) 177–186. doi:10.14359/51685532.
- [40] ASTM C496, Standard Test Method for Splitting Tensile Strength of Cylindrical Concrete Specimens ASTM C-496, ASTM International, West Conshohocken (PA), USA, 2011. doi:10.1520/C0496.
- [41] ASTM C1856, Standard Practice for Fabricating and Testing Specimens of Ultra-High Performance Concrete, ASTM International, West Conshohocken, PA, USA, 2017.
- [42] ASTM C469, Standard Test Method for Static Modulus of Elasticity and Poisson’s Ratio of Concrete in Compression, ASTM International, West Conshohocken (PA), USA, 2014. doi:10.1520/C0469.
- [43] I. De la Varga, B.A. Graybeal, Dimensional Stability of Grout-Like Materials Used in Field-Cast Connections (No. FHWA-HRT-16-080), McLean, VA, 2016.

## **7. Acknowledgements**

The research presented in this paper was funded by the U.S. Federal Highway Administration. The publication of this paper does not necessarily indicate approval or endorsement of the findings, opinions, conclusions, or recommendations either inferred or specifically expressed herein by the Federal Highway Administration or the United States Government.